Title

10 MeV PROTON REACTION CROSS SECTION

Authors

Igo, G.
Wilkins, B.

Publication Date

1962-09-26

UCRL-10480

University of California

Ernest O. Lawrence Radiation Laboratory

Berkeley, California

DISCLAIMER

Submitted for Pub. in Physics Letters

UCRL-10480

UNIVERSITY OF CALIFORNIA
Lawrence Radiation Laboratory
Berkeley, California
Contract No. 7405-eng-48

10 MeV PROTON REACTION CROSS SECTIONS

G. Igo and B. Wilkins

September 26, 1962

10 MeV PROTON REACTION CROSS SECTIONS

G. Igo and B. D. Wilkins

Lawrence Radiation Laboratory
University of California
Berkeley, California

September 26, 1962

Proton reaction cross sections measured at energies near the coulomb barrier height should be sensitive to the nuclear potential. Small variations in barrier height due to the shape and character of the nuclear potential can alter the reaction cross section by a large amount. We therefore have obtained proton nonelastic cross sections near 10 MeV from Be, C, Al, Ti, Mo, Zr, Fe, Ni, Zn, Cu, V, Rh, Nb, Ag, Sn, Ta, Th, Au, and Pb.

The most significant features of the data are the appearance of a minimum in the vicinity of nuclei with $Z = 28$ protons, an anomalously low cross section for carbon, and a systematic deviation from optical model predictions[1,2] for heavier elements.

The beam preparation is shown schematically in Fig. 1, and the parameters for the proton measurements are quoted below. The external beam from the 60-inch cyclotron is focused by a quadrupole and a bending magnet on a 1/8 in. diameter tantalum collimator slightly thicker than the range of the ion in the beam and followed by an antiscattering baffle. This beam was incident on a scattering foil that for some measurements was a lead foil enriched in Pb^{208} ($\Delta E \approx 1.0$ MeV for 12-MeV H^+ ions) and a thorium foil of approximately the same stopping power for the rest of the measurements.

Scattered particles at 15° can pass through a collimating system consisting of two anti-wall scattering baffles and then through a 0.062-in.-collimator placed 10 in. from the lead foil followed by an antiscattering baffle. The collimated beam produced by this system passes through two 3-mil-thick plastic scintillators (counter 1 and counter 3) spaced 22 in. apart.

In order to remove protons multiply-scattered away from the axis of the beam line, a 0.180-in.-plastic scintillator collimator counter (counter 2) was placed directly in front of counter 3. Counter 1 and counter 3 output pulses were put into fast coincidence ($\tau \approx 2$mμ sec), and pulses from counter 2, after having passed through a tunnel diode discriminator circuit[3] that produces shaped pulses of uniform height and of width 20 mμsec, were put into anticoincidence.

Counter 4 is a 4-in.-long cylinder of plastic scintillator with a 0.3-in. wall thickness and an inner diameter of 0.20-in. It is viewed by a 6810 photomultiplier, and it serves further to collimate the beam, since some particles are multiply-coulomb scattered out of the beam line in counter 3. Counter-4 pulses also pass through a tunnel diode discriminator circuit and are put into anticoincidence. Finally, then, a beam particle is defined by an event of the kind $1\,\bar{2}\,3\,\bar{4}$, and in what follows we understand that the intensity I_0 represents the frequency of events of this kind, i.e. $I_0 = 1\,\bar{2}\,3\,\bar{4}$. In the attenuation technique utilized here the quantity I_0-I is measured by placing counter 5 (see Fig. 1) in anticoincidence, i.e., $I_0 - I = 1\,\bar{2}\,3\,\bar{4}\,\bar{5}$. The advantage of this kind of measurement over measuring I_0 and I separately is obvious.

At the beam levels used in this experiment, significant gain shifts in counter 5 are to be expected. It is therefore extremely difficult to eliminate inelastic events occurring in the target by pulse-height analysis. A simpler and reliable way is to place an energy-degrading foil in front of counter 5 thick enough to stop protons that have been inelastically scattered in the target. In practice the degrader was adjusted so that 6.5-MeV protons produced by inelastic events at the center of the target (thickness ≈ 1 MeV) were unable to pass through the degrader.

Absorption of the protons occur more frequently in the Al degrader, since it is several times as thick as the targets. This contribution had to be subtracted. This is done by removing the target and placing a "dummy" target in the beam ahead of the scattering foil of such a thickness that the beam energy incident on the degrader foil is the same, and the numbers of i_0 ($= 1\,\bar{2}\,3\,\bar{4}$) and $i_0 - i$ ($= 1\,\bar{2}\,3\,\bar{4}\,\bar{5}$) events are measured.

Combining the results of this measurement and the elastic scattering data,[4,5,6,7] we obtain the quantity

$$\sigma_R - \sigma_{CE} - \int_0^{\theta_5} \sum_{i=1}^{N} \sigma_i(\theta)\, d\Omega,$$

where σ_{CE} is the compound elastic cross section, σ_R is the reaction cross section, $\sigma_i(\theta)$ is the differential cross section for inelastic scattering to the ith excited state, N is the highest excited state from which inelastic protons may pass through the degrader, and θ_5 is the angle subtended by counter 5 at the target.

As we improve the energy resolution, the inelastic scattering term may be reduced but σ_{CE} remains. It may be large compared with the value of σ_R at low energies for light targets. At high energies it generally will be of negligible importance. For the 10-MeV proton measurements, the compound elastic correction may be very large. Since the inelastic-scattering term can be estimated from inelastic-scattering data,[8] the extracted quantity is $\sigma_R - \sigma_{CE}$, the nonelastic cross section. It should be noted that optical-model calculations generally predict σ_R.

In Fig. 2 the predicted reaction cross sections σ_R at 10 MeV for a surface absorption potential[1] that fit the elastic-scattering data are plotted. Also plotted are the measured values of $\sigma_R - \sigma_{CE}$. The agreement with the results from the surface-absorption model is qualitatively good for $A^{2/3} > 16$

(where A is the atomic mass), although the measured values tend to be systematically larger. The solid and dashed curves representing the optical-model predictions show the change in the cross section resulting from the beam energy difference on the two experimental runs when the data were collected. The experimental points systematically reflect a similar difference. For $A^{2/3} < 16$, the strong minima near Ni and C cause large deviations from the predictions, but it should be emphasized that we measure $\sigma_R - \sigma_{CE}$. It is quite possible that these deep minima may be due to resonances in σ_{CE} near C and Ni. Such an interpretation of neutron reaction cross-section data has been suggested by Perey.[9] At 10 MeV, C is certainly expected to have a large cross section for σ_{CE}. Because of the high (p,n) threshold, 18 MeV, only two states, the ground state and the first excited state, are appreciably populated from the compound nucleus at 10 MeV.[10] One expects these states to be roughly of equal intensity, thus explaining the deep minimum we get in $\sigma_R - \sigma_{CE}$ for C.

An alternative viewpoint, that the minimum in the vicinity of Ni is associated with σ_R, cannot be ruled out. This would imply that the nuclear area presented to the projectile shrinks by about 12% in the vicinity of the proton closure at 28 protons, or a size resonance occurs.[11] Measurements of 40-MeV alpha-particle reaction cross sections (soon to be reported) also show a minimum near Z = 28. This tends to support the viewpoint that the nucleus shrinks there, since σ_{CE} should be insignificant at 40 MeV for alpha particles and size resonances should have a small effect.

Figure 3 shows the predicted range of values for the reaction cross section by use of a Woods-Saxon potential (volume absorption) adjusted to fit the elastic-scattering data. The experimental reaction cross section is not inconsistent with the upper limit predicted by volume absorption. Note in Fig. 3 that the calculations were for specific elements.[2,12] As an example, the range of reaction cross sections predicted as in Fig. 7 in the vicinity of $A^{2/3} = 16$ should be compared with the Cu data point and not with the experimental measurements for nearby elements. For larger values of $A^{2/3}$ the shaded bar represents only regions where good fits could be obtained and does not necessarily represent limits of σ_R. Although greatly restricting the sets of parameters that one may use, the σ_R data have not yet enabled one to choose between surface and volume absorption.

REFERENCES

1. F. Bjorklund and S. Fernbach, Phys. Rev. 109, 1295 (1958).
2. A. E. Glassgold, W. B. Cheston, M. L. Stein, S. B. Schuldt, and G. W. Erickson, Phys. Rev. 106, 1207 (1957).
3. A. E. Bjerke, Q. A. Kerns, and T. A. Nunamaker, Lawrence Radiation Laboratory Report UCRL-9838, 1961.
4. N. M. Hintz, Phys. Rev. 106, 1201 (1957).
5. Y. Nagahara, J. Phys. Soc. Japan 16, 133 (1961).
6. K. Kikuchi, S. Kobayashi, and K. Matsuda, J. Phys. Soc. Japan 14, 121 (1959).
7. C. Hu, K. Kikuchi, S. Kobayashi, K. Matsuda, Y. Nagahara, Y. Oda, N. Takano, M. Takeda, and T. Yamazaki, J. Phys. Soc. Japan 14, 861 (1959).
8. N. M. Hintz (University of Minnesota), private communication.
9. F. G. J. Perey (Oak Ridge National Laboratory), private communication.
10. H. E. Conzett, Phys. Rev. 105, 1324 (1957).
11. J. Wing and J. R. Huizenga, (p,n) Cross Sections of V^{51}, Cr^{52}, Cu^{43}, Cu^{65}, Ag^{107}, Ag^{109}, Cd^{111}, Cd^{114}, La^{139} from 5 to 10.5 MeV, submitted to Phys. Rev.
12. J. S. Nodvik and D. S. Saxon, Phys. Rev. 117, 1539 (1960).

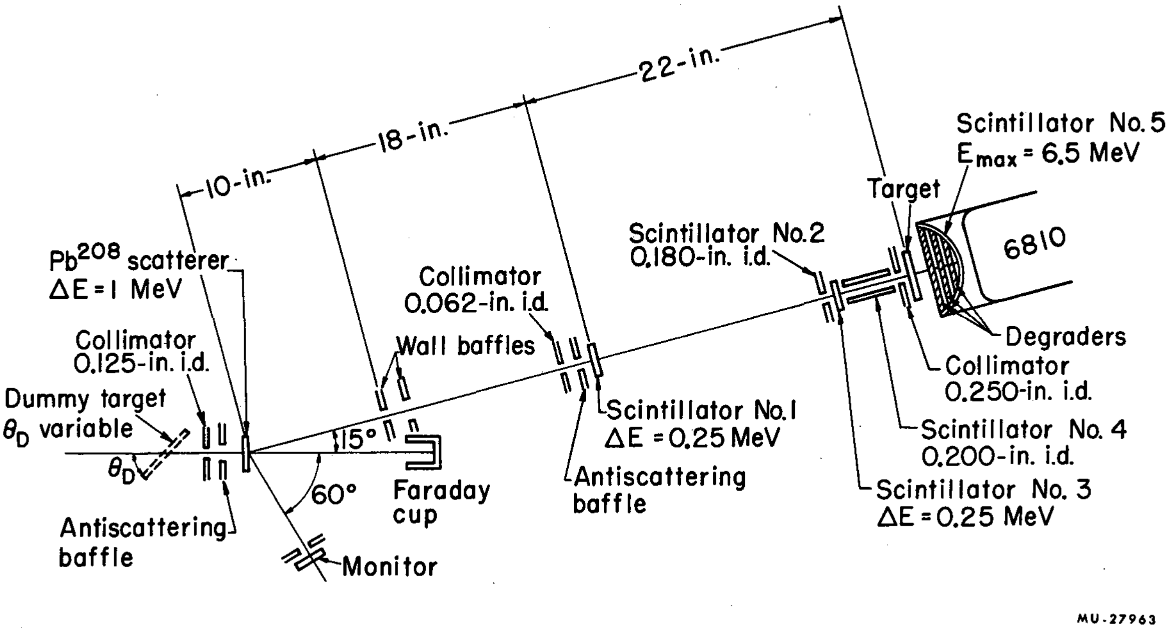

Fig. 1. Schematic diagram of the experimental area.

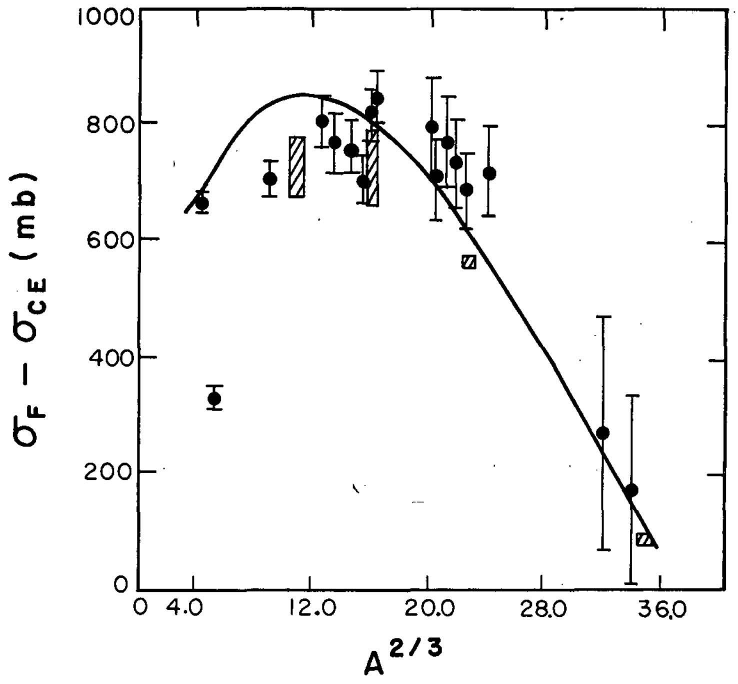

Fig. 2. Proton σ_R - σ_{CE} around 10 MeV: ● - the experimental points at 10.1 to 10.2 MeV, ■ - the experimental points at 9.9 to 10.0 MeV. The solid and dashed curves are the theoretical predictions of σ_R at 10.1 and 9.9 MeV, using an optical model with surface absorption.[9,15]

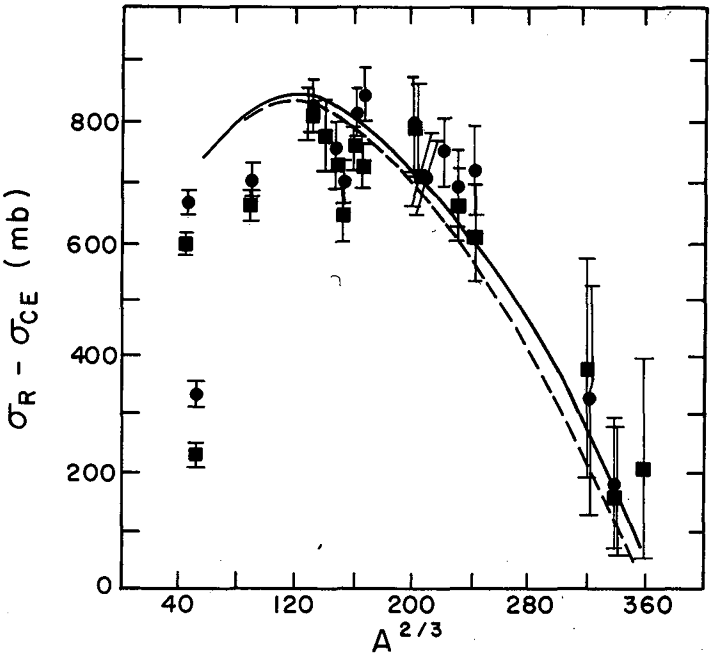

MU-27135

Fig. 3. Proton reaction cross sections showing predictions using both volume and surface absorption. The symbol ⧳ represents the experimental points; the solid curve, surface absorption predictions of Bjorklund and Fernbach; and ▨, range of values predicted by the Woods-Saxon potential (volume absorption) as calculated by Glassgold et al.[2] and Nodvik and Saxon.[12]

[illegible] و [illegible]